Stability of Highly Shifted Equilibria in a Large-Aspect-Ratio Tokamak

P.-A. Gourdain, S. C. Cowley, J.-N. Leboeuf, and R. Y. Neches
Department of Physics and Astronomy, University of California Los Angeles, California 90095-1547, USA
(Received 6 May 2006; published 4 August 2006)

High beta poloidal tokamaks can confine plasma pressures an order of magnitude higher than their low beta poloidal counterparts. The theoretical stability of these high beta poloidal magnetohydrodynamics equilibria was left unresolved for many years. Using modern computational tools, such configurations are now found stable to Mercier, resistive and high-n (ideal and resistive) ballooning criteria as well as fixed and free-boundary modes for a wide range of current density profiles in the framework of a low field large-aspect-ratio machine.

DOI: 10.1103/PhysRevLett.97.055003 PACS numbers: 52.55.Tn, 52.30.Cv, 52.55.Fa

The most promising magnetic fusion concept is an axisymmetric configuration called a tokamak, where a plasma (i.e., ionized gas) is confined by an external magnetic field and a toroidal electrical current running through the plasma itself. The plasma geometry looks like a torus with arbitrary cross section. The confinement efficiency is measured by means of a simple figure of merit called the plasma beta, β. This is the ratio of the kinetic pressure and the magnetic pressure

$$\beta = 2\mu_0 \frac{p}{B^2}. \quad (1)$$

B is the total magnetic field confining the plasma of pressure p. Since this field is the main cost of the device, high β plasmas lead to the design of cost effective machines. Another efficiency parameter is the poloidal beta, β_p,

$$\beta_p = 2\mu_0 \frac{\langle p \rangle}{\langle B_p^2 \rangle}, \quad (2)$$

where B_p is the magnetic field created by the toroidal plasma current. β_p is solely dependant on the current distribution inside the plasma. In ideal magnetohydrodynamics (MHD) theory, the pressure is maximum where B_p is null. This location is called the magnetic axis. If β_p is close to 0, the axis is near the geometrical center of the plasma cross-section. As β_p increases (but not necessarily β), the axis moves towards the plasma edge. Figure 1(a) shows the major difference between standard and asymptotic (i.e., extremely shifted) configurations. The lines represent the surfaces of constant poloidal magnetic flux created by B_p, or flux surfaces, which are also surfaces of constant plasma pressure p. This shift is called the Shafranov shift, measured relative to the plasma minor radius, a. The control of the plasma shape for large shifts is mandatory to obtain equilibria that are not wall-confined. By using an external set of coils to shape the plasma boundary, the cross section of the plasma will stay circular independently of the Shafranov shift. When no shaping coils are used, an X point appears on the high field side of the plasma due to the strong vertical field necessary to confine the plasma inside the vacuum chamber. This limits the shift to a value of approximately 50%, well below the value presented in this Letter. The pressure gradient in such devices is confined by the Lorentz force. This MHD equilibrium obeys

$$\nabla p = J \times B. \quad (3)$$

J is the toroidal plasma current density (hereafter "current density" or "current" in this Letter). By increasing J,

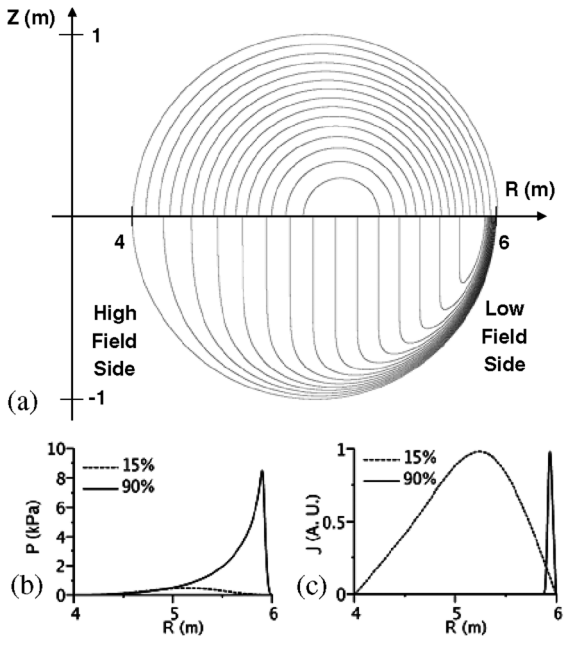

FIG. 1. (a) Flux surfaces for a circular plasma cross section. The Z axis is the axis of axisymmetry (actually located at $R = 0$). Because of the up-down symmetry, only one half of the configurations are shown. The top set of surfaces is for a 15% Shafranov shift ($\beta = 1.8\%$, $\beta_p = 1.15$) and the lower set of surfaces represents an equilibrium with a 90% shift ($\beta = 35\%$, $\beta_p = 50$). The magnetic axis is located on the plane of symmetry ($Z = 0$) at $R = 5.15$ m (15% shift) and $R = 5.90$ m (90% shift). (b) Pressure and (c) normalized current density profiles for the same shifts.

larger pressure gradients can be confined. Unfortunately, increasing J decreases the safety factor q, which should always remain above 1. This requirement limits the maximum current density that can be sustained in a tokamak without creating unrecoverable MHD instabilities, called internal kinks. As a result, conventional tokamak designs are low β.

When a shifting of the axis occurs the current density J can be increased significantly before the minimum value of the safety factor drops below 1. Thus, for the same confining magnetic field, high β_p machines can confine higher pressures than their low β_p counterparts, as illustrated by Fig. 1(b). The Shafranov shift alters the shape of the flux surfaces but also the current density distribution. It produces a shifted, sharp peak in the current density profile [Fig. 1(c)]. It was assumed that the presence of these large gradients would trigger major MHD instabilities, which explains the lack of interest in the topic despite its obvious attractive properties. Nevertheless, analytic asymptotic equilibria ($\beta_p \gg 10$) [1] were shown to be stable to several MHD instabilities, such as localized ballooning, interchange, and internal kink modes in large-aspect-ratio machines [2,3].

With new computational tools, a thorough study of ideal MHD stability can now be conducted, focusing on Mercier [4], Glasser-Greene-Johnson (GGJ) resistive [5] and high-n (ideal or resistive) ballooning [6,7] criteria as well as the stability of ideal MHD modes with low toroidal mode numbers ($n = 1, 2, 3$) for fixed and free-boundary equilibria. Ballooning modes are a localized instability driven by pressure gradients in the plasma. They usually have a large toroidal mode number n and can be driven by ideal or resistive phenomena. The Mercier instability is the limiting case of ballooning modes, historically discovered before the generalized criterion previously discussed. The GGJ criterion evaluates the resistive interchange instabilities, which tend to eliminate the stabilizing influence of magnetic shear on ideal MHD interchanges. Using these different criteria, we investigate here the stability of several current density profiles. All current shapes have a large portion of their profiles equal to zero, which enforces large shifts. In the region where $J = 0$, Eq. (3) is satisfied since diamagnetic poloidal plasma currents equilibrate pressure gradients. In order to understand the stability dependence of large β_p, we scanned various current density profile shapes. To constrain the parameter space, all scans used the geometry and magnetics of the Electric Tokamak (ET). ET has a major radius $R = 5$ m, a minor radius $a = 1$ m, a toroidal field $B_t = 0.25$ T and a total plasma current $I_P = 50$ kA [8]. It is a large-aspect ratio, low field device with a circular cross section. These properties tend to minimize the geometric and magnetic effects on stability. To accomplish this theoretical study, the high β free-boundary code CUBE [9] was used to generate high resolution equilibria. This code uses a multigrid approach and a plasma current density constraint to obtain convergence at high beta. A dozen of external coils is uniformly distributed around the computational grid and constrains the plasma shape and position for any β_p. To determine stability, we used the DCON code, which solves the Euler-Lagrange equation to minimize the potential energy and evaluates a real critical determinant whose poles indicate the presence of ideal instabilities [10]. Previous high β_p equilibrium codes [11] were low resolution and incompatible with stability code requirements. Three different types of shape modifications are studied; the radial position of the current peak [Fig. 2(a)], the current profile peaking [Fig. 2(b)], and the transition between the null and non-null current regions [Fig. 2(c)]. All profiles presented have a Safranov shift of about 80%, and are Mercier stable. The rest of this Letter will focus on current profile shape changes which lead to other types of instabilities.

Our first treatment of the stability properties for highly shifted configurations focuses on the effects of the location of the current peak. The resulting shape modifications are indicated in Fig. 2(a). Profile A has a central q just below 1 and limits the scan on the magnetic axis side. As the peak

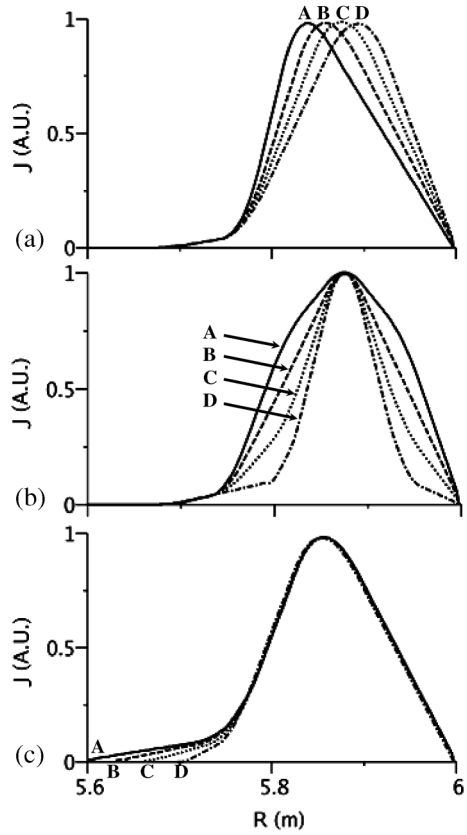

FIG. 2. Current profile scans used in the stability study of high β_p equilibria. (a) Peak position, (b) peaking factor, (c) current profile transition scans. The plasma extends from $R = 4$ m to $R = 6$ m. Part of the null region of the current profile has been truncated from the plots to enlarge the section where shape changes occur. The magnetic axis is located around $R = 5.80$ m.

moves to the low field side of the plasma β decreases while the whole q profile rises. Figure 3(a) shows the different criteria as a function of the normalized radius, $\rho = r/a$. In this parameter scan, the only concern lies with resistive instabilities which emerge as the peak of the profile moves away from the magnetic axis. The high-n ballooning criterion is never violated in this scan. In fact, the peak location does not alter this criterion in a meaningful manner. We observe that relatively large swings of the current profile peak are not likely to push the equilibrium into an unstable regime of operation. The stability is theoretically guaranteed for all profiles bounded by profiles B and C. The safety margin on the GGJ criterion between stable and unstable regions is large enough to insure robust stability across the whole profile. Moreover, the large swing in peak position barely affects the Shafranov shift which varies by less than a percent. Lastly, all profiles are stable to all fixed-boundary modes with toroidal numbers $n = 1, 2, 3$.

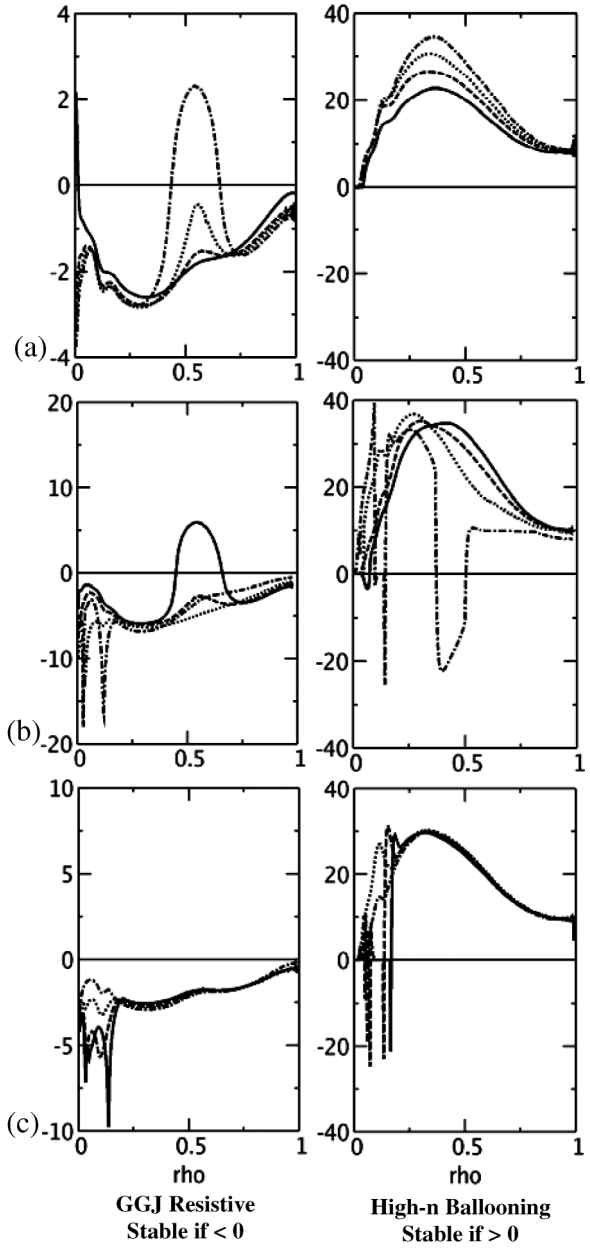

FIG. 3. GGJ resistive and high-n ideal ballooning criteria of profiles A (solid lines), B (dashed lines), C (dotted lines), and D (dash-dot lines) for (a) peak location, (b) peaking factor, and (c) transition scans. The different criteria are plotted as a function of ρ ($=r/a$). $\rho = 0$ is at the magnetic axis and $\rho = 1$ at the plasma edge. The ordinates of all curves are in arbitrary absolute units. In the left column, the part of the profiles that is positive shows instabilities to resistive interchange instabilities. In the right column, the profiles are stable if the criterion is positive.

After investigating the effects of the peak position on stability, we turn to the shape of the current peak itself. The different profiles investigated are collected in Fig. 2(b). Profile D is particularly interesting because the strong peaking in current density significantly increases the pressure that can be confined. Since we keep the total plasma current constant, peaked profiles have high current densities. The width of the current density peak influences the pressure and q profiles in a large region surrounding the magnetic axis. Figure 3(b) regroups the stability results for this scan. The peaked current profile D suffers from high-n ballooning instabilities. Broad profiles such as profile A are impervious to ballooning modes, but are bedeviled by resistive instabilities in a large region of the plasma. Broad profiles also lower the effective plasma pressure, which makes them less attractive. Profiles B and C have acceptable stability and average β. These two profiles are our current shape references. All profiles are stable to the fixed-boundary modes with $n = 1, 2$ and 3. Profile C is also stable to free-boundary modes for $n = 1$, 2, and 3.

The shape of the transition region, where the null toroidal current ends and the strong current gradient begins, is now studied. Figure 2(c) presents the different cases investigated. The interplay between the transition, pressure and q profiles remains strongly localized to the magnetic axis. A gentle transition (profile A of Fig. 2(c)] increases the value of q at the axis. The reduction in magnetic shear triggers high-n ballooning modes [12], as highlighted by Fig. 3(c). Nevertheless, the localization of high-n ballooning modes around the magnetic axis does not jeopardize overall plasma stability. When a sharp transition [profile D of Fig. 2(c)] appears, the resistive criterion degrades and further steepening will yield resistive instabilities. Finally, all the profiles investigated are stable to fixed-boundary modes ($n = 1, 2, 3$).

While the majority of equilibria presented in Fig. 2 are stable to ideal ballooning modes, resistive ballooning modes may be unstable in the so-called first stability regime [13], where the shear s is comparable to the normalized pressure gradient α, using

$$s = \frac{r}{q}\frac{dq}{dr} \quad \text{and} \quad \alpha = -2\mu_0 \frac{Rq^2}{B_t^2}\frac{dp}{dr}. \tag{4}$$

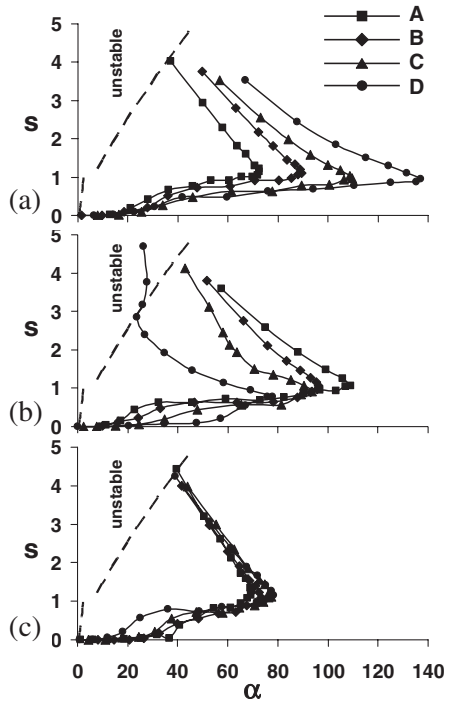

FIG. 4. s-α diagrams for (a) peak, (b) peaking factor, and (c) transition scans. The majority of profiles are in the second stability regime for high-n resistive ballooning modes. The diagrams exclude the region above q_{95}.

In contrast, equilibria in the second stability regimes ($s \ll \alpha$) are usually stable to resistive ballooning modes [14]. Ideal and resistive ballooning limits merge for low s and α, as occurs in the plasma core. Examining ideal ballooning stability instead is usually acceptable in this region. In contrast, these limits diverge for larger values of s and α in the plasma mantle ($r/a > 0.5$). The s-α diagram must be used to assess the high-n resistive ballooning mode stability directly. Figure 4 shows that all the profiles presented in this Letter are in the second stability regime and they are stable to resistive ballooning modes, except for extremely peaked profiles [such as profile D from Fig. 2(b)]. If the location of the current peak is close to the magnetic axis, as for profile A from Fig. 2(a), the stability to resistive ballooning modes is marginal at the plasma edge. On the other hand, the transition from null to high current density does not affect the s-α curves in either critical region of the diagram. High-n resistive ballooning stability remains unaffected.

The stability of highly shifted configurations using ET geometry and magnetics has been studied in this Letter. Detailed scans of the current profile shape revealed that robust stability exists for a wide range of contiguous profiles. While keeping geometric and magnetic parameters constant, a systematic study demonstrated that a wide range of shifted equilibria are stable according to Mercier, GGJ resistive, and high-n ballooning criteria. Furthermore, fixed-boundary modes with toroidal mode numbers $n = 1$, 2, and 3 are stable in all the cases explored. This work extends and completes previous analytic and asymptotic research on the stability of equilibria with large Shafranov shifts [2,3]. The impact of current density peak location, profile peaking, and transition on the stability was investigated. Peak location affects the stability by degrading the GGJ resistive criterion or by lowering the central q below 1. The peaking factor is an important parameter in the stability of the equilibria. Unlike peak location, profile peaking triggers both ballooning as well as resistive instabilities. Finally, although a current profile transition may trigger ballooning modes, in this case they should raise few concerns for stability because they are localized to the magnetic axis. Smooth current profiles without any of these extreme characteristics are stable to major ideal MHD instabilities in high β_p regimes. The target profile for a high β_p device should correspond to current density C of Fig. 2(b). This current distribution is stable according to all classical ideal MHD criteria as well as to resistive high-n ballooning modes. It is also stable to all fixed and free-boundary modes with toroidal mode numbers $n = 1$, 2, or 3.

One of the authors (P.-A. G.) would like to thank Dr. R. J. Taylor for contributing computational resources used in this study, and Dr. A. H. Glasser for providing his DCON code. This research was funded by DOE Grants No. DE-FG02-04ER54737 and No. DE-FG02-04ER54740.

[1] S. C. Cowley *et al.*, Phys. Fluids B **3**, 2066 (1991).
[2] S. C. Cowley, Phys. Fluids B **3**, 3357 (1991).
[3] O. A. Hurricane, B. D. G. Chandran, and S. C. Cowley, Phys. Plasmas **7**, 4043 (2000).
[4] C. Mercier, Nucl. Fusion **1**, 47 (1960).
[5] A. H. Glasser, J. M. Greene, and J. L. Johnson, Phys. Fluids **18**, 875 (1975).
[6] J. W. Connor, R. J. Hastie, and J. B. Taylor, Phys. Rev. Lett. **40**, 396 (1978).
[7] H. P. Furth *et al.*, Plasma Phys. Controlled Nucl. Fusion Res. **I**, 103 (1966).
[8] R. J. Taylor *et al.*, Nucl. Fusion **42**, 46 (2002).
[9] P.-A. Gourdain, J.-N. Leboeuf, and R. Y. Neches, J. Comput. Phys. **216**, 275 (2006).
[10] A. H. Glasser, The direct criterion of Newcomb (DCON) for the stability of an axisymmetric toroidal plasma, Los Alamos Report No. LA-UR-95-528, 1997.
[11] P.-A. Gourdain and J.-N. Leboeuf, Phys. Plasmas **11**, 4372 (2004).
[12] J. W. Connor and R. J. Hastie, Phys. Rev. Lett. **92**, 075001 (2004).
[13] H. R. Strauss, Phys. Fluids **24**, 2004 (1981).
[14] A. Sykes, C. M. Bishop, and R. J. Hastie, Plasma Phys. Controlled Fusion **29**, 719 (1987).